

## Supplementary information

### **Stereolabile Chiral Biphenyl Hybrids: Crystallization-Induced Dynamic Atropselective Resolution Involving Supramolecular Interactions**

Chi-Tung Yeung,<sup>a</sup> Ho-Lun Yeung,<sup>a</sup> Wesley Ting Kwok Chan,<sup>a</sup> Siu-Cheong Yan,<sup>a</sup> Eric C. Y. Tam,<sup>b</sup> Ka-Leung Wong,<sup>c</sup> Chi-Sing Lee<sup>d</sup> and Wing-Tak Wong<sup>a,\*</sup>

<sup>a</sup>*State Key Laboratory for Chirosciences, Department of Applied Biology and Chemical Technology, The Hong Kong Polytechnic University, Hung Hom, Hong Kong SAR. Tel: 852 3400 8789; E-mail: [bcwtwong@polyu.edu.hk](mailto:bcwtwong@polyu.edu.hk)*

<sup>b</sup>*Department of Chemistry, University of Sussex, Falmer, Brighton BN1 9QJ, UK.*

<sup>c</sup>*Department of Chemistry, The Hong Kong Baptist University, Kowloon Tong, Hong Kong SAR.*

<sup>d</sup>*Laboratory of Chemical Genomics, School of Chemical Biology and Biotechnology, Peking University Shenzhen Graduate School, Shenzhen University Town, Xili, Shenzhen 518055, China.*

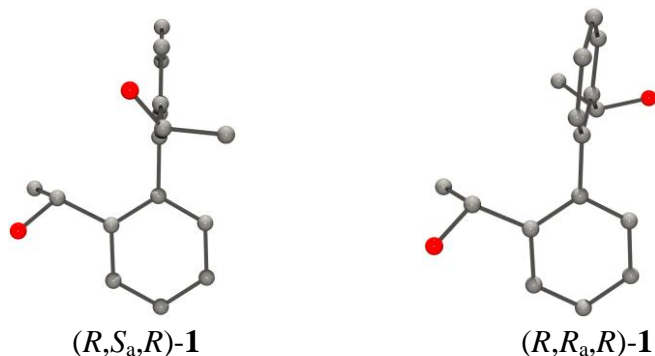
#### **1. DFT calculations for 1–3**

All computational calculations on the gas-phase molecules were carried out using the density functional theory (DFT) in the Gaussian 03w program package (version E.01), performed at B3LYP level with 6-31g(d) basis set for all atoms [default parameters were used throughout].<sup>1</sup> The geometry optimizations were performed using the parameters from the crystal structures, where possible, as a starting point and their local minima were verified by the absence of imaginary frequencies. Zero-point vibrational frequencies were calculated on the optimized structures [default conditions were used: pressure at 1 atm and temperature at 298.15 K]. Thermodynamic data were extracted from the zero-point vibrational energy calculations.

### DFT result on **1**

Gaussian version: E.01

Basis set: DFT B3LYP/6-31g(d)



The input parameters for optimization on  $(R,S_a,R)$ -1 is based on crystallographic data. Results for **1** are summarized in Table S1:

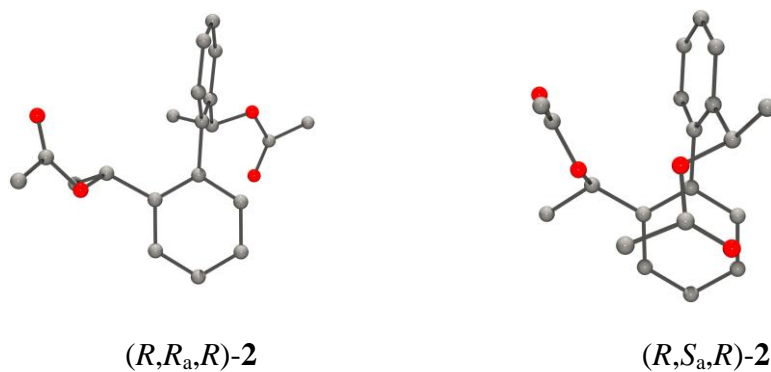
Table S1. Energy difference between  $(R,S_a,R)$ -1 and  $(R,R_a,R)$ -1

	$(R,S_a,R)$ -1 (hartree)	$(R,R_a,R)$ -1 (hartree)	energy difference (kcal/mol)
HOMO-LUMO energy gap	0.2768	0.277	-0.14
Zero-point energy	-770.6742	-770.672	1.38
Enthalpy	-770.6561	-770.6539	1.38
Free energy	-770.7197	-770.7179	1.16

### DFT result on **2**

Gaussian version: E.01

Basis set: DFT B3LYP/6-31g(d)



The input parameters for optimization on  $(R,R_a,R)$ -2 is based on crystallographic data. Results for **2** are summarized in Table S2:

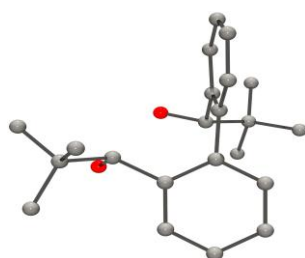
Table S2. Energy different between  $(R,R_a,R)$ -**2** and  $(R,S_a,R)$ -**2**

	$(R,R_a,R)$ - <b>2</b> (hartree)	$(R,S_a,R)$ - <b>2</b> (hartree)	energy difference (kcal/mol)
HOMO-LUMO energy gap	0.2583	0.2573	0.63
Zero-point energy	-1075.9373	-1075.9336	2.32
Enthalpy	-1075.9122	-1075.9094	1.75
Free energy	-1075.9943	-1075.9869	4.64

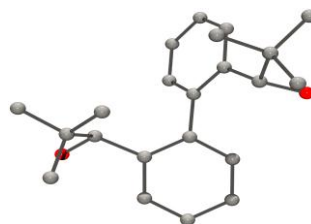
### DFT result on **3**

Gaussian version: E.01

Basis set: DFT B3LYP/6-31g(d)



$(S,R_a,S)$ -**3**



$(S,S_a,S)$ -**3**

The input parameters for optimization on  $(S,R_a,S)$ -**3** is based on crystallographic data. Results for **3** are summarized in Table S3:

Table S3. Energy difference between  $(S,R_a,S)$ -**3** and  $(S,S_a,S)$ -**3**

	$(S,R_a,S)$ - <b>3</b> (hartree)	$(S,S_a,S)$ - <b>3</b> (hartree)	energy difference (kcal/mol)
HOMO-LUMO energy gap	0.2633	0.2703	4.39
Zero-point energy	-1006.3817	-1006.3712	6.59
Enthalpy	-1006.3561	-1006.3453	6.78
Free energy	-1006.4344	-1006.4244	6.28

## 2. Solution state studies on **1**

### a. Chemical shifts of Hydroxyl protons of **1** in $\text{CDCl}_3$

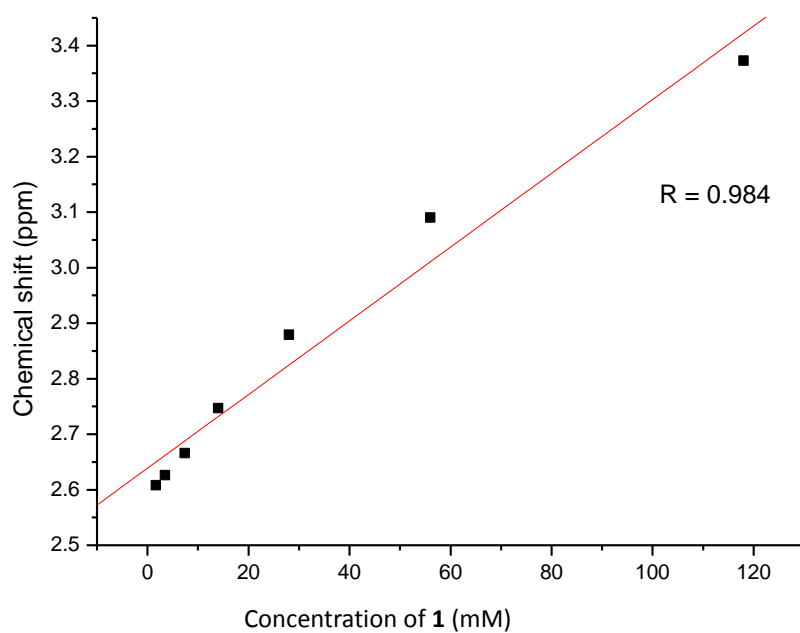


Fig. S1: Concentration dependence of chemical shift of the hydroxyl proton of **1** in  $\text{CDCl}_3$

### b. Circular dichroism spectrum of **1**

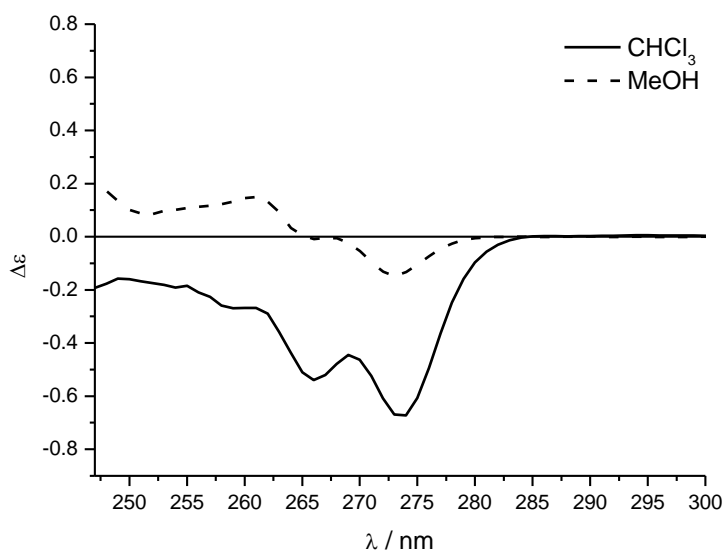


Fig. S2. Circular dichroism spectrum of **1** in  $\text{CHCl}_3$  and MeOH ( $c$  0.0323 M, path 0.1cm)

### c. The Diffusion Ordered Spectroscopy (DOSY) of **1** in CDCl<sub>3</sub>

Diffusion ordered spectroscopy was performed at 25 °C, using 2 mg of heptakis(2,3,6-tri-*O*-methyl)- $\beta$ -cyclodextrin (MW = 1429 gmol<sup>-1</sup>) as internal standard in CDCl<sub>3</sub>.<sup>2,3</sup> Ratios of diffusion coefficients of **1** to the standard were found to increase from 0.21 to 0.27 when concentrations of **1** were decreased from 118 mM to 1.85 mM.

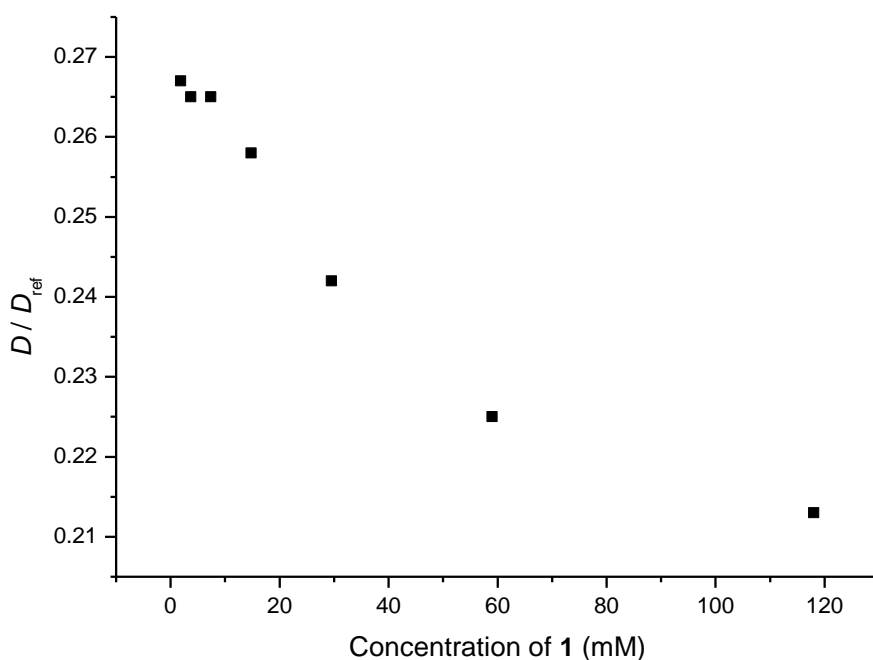


Fig. S3. Concentration dependence of relative diffusion coefficient of **1** to internal reference (heptakis(2,3,6-tri-*O*-methyl)- $\beta$ -cyclodextrin, physical separated) in CDCl<sub>3</sub> at 25 °C.

## 3. Experimental

### General

(*R*)-2-bromo- $\alpha$ -methylbenzenemethanol,<sup>4</sup> oxazaborole-borane catalyst = (*S*)-tetrahydro-1-methyl-3,3-diphenyl-1*H*,3*H*-pyrrolo[1,2-*c*][1,3,2]oxazaborole-Borae<sup>5</sup> and 1-(2-bromophenyl)-2,2-dimethylpropanone<sup>6</sup> were prepared accordingly to literatures respectively. Solvent were dried using an appropriate drying agent when required (Hexane over sodium, THF and diethyl ether over Na/benzophenone, dichloromethane over calcium hydride). Dimethylformamide (DMF) was commercially available in anhydrous condition. All other chemicals were purchased commercially and used as received. Unless otherwise stated, all manipulations were

carried out under nitrogen using standard Schlenk line technique. Merck silica gel 60 (70–230 mesh) was used for column chromatography. NMR spectra were recorded on a Bruker Ultrashield Advance Pro 400 MHz instrument and the chemical shifts were referenced internally to tetramethylsilane (TMS) in parts per million (ppm). The enantiomeric excess of the alcoholic intermediates were determined by HPLC with a Daicel Chiralcel OJ-H or Regis (S,S) Whelk-O1 (4.6mm X 250 mm, 5 $\mu$ m particle size). The enantiomeric purity was compared with a racemic mixture according to the elution orders. The absolute configuration was determined with X-ray crystallography. CD spectra were recorded with a Jasco J-801 spectropolarimeter with a 1 mm cell at 25 °C and presented as  $\Delta\epsilon$  in M<sup>-1</sup>cm<sup>-1</sup>.

### X-ray crystallography

Measurements of crystal data were carried out on a Bruker Smart 1000 system equipped with an APEX II CCD device for **1–3**, *rac-1* and (*S*)-1-(2-bromophenyl)-2,2-dimethylpropan-1-ol with graphite monochromated Mo-K $\alpha$  radiation at room temperature. Multi-scan absorption correction was applied by SADABS program,<sup>7</sup> and the SAINT program was utilized for integration of the diffraction profiles.<sup>8</sup> The structures were solved by direct method and was refined by a full matrix least-squares treatment on  $F^2$  using the SHELXTL programme system.<sup>9,10</sup> Structure *rac-1* contains a highly disordered lattice solvent (CDCl<sub>3</sub>), and was removed from the refinement using the PLATON/SQUEEZE program.<sup>11</sup> Crystal data, as well as details of data collection and refinement, are summarized in Table S1 and S2. Crystallographic data for the structural analysis has been deposited with Cambridge Crystallographic Data Centre, CCDC No. 845646 for **1**; No. 845648 for **2**; No. 845647 for **3**; No. 894349 for *rac-1*; No. 894348 for (*S*)-1-(2-bromophenyl)-2,2-dimethylpropan-1-ol.

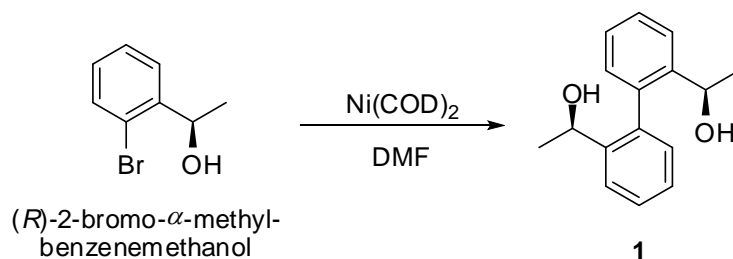
### H-atoms refinement

Proton refinements were performed through a number of ways for the structures reported in this manuscript. All carbon-bonded protons were refined using their respective riding model. Initially, attempts were made to locate hydroxyl protons using the Fourier difference map, with varying degree of success. A few hydroxyl protons could not be accurately located by means of Fourier synthesis due to a number of factors, namely the nature of proton in relation to single crystal X-ray crystallography, quality of data, and also disordering. These protons were refined using the theoretical riding model. Rotational disorder affects almost all hydroxyl protons. Hydrogen bondings in these structures can take up different orientations, meaning that the hydroxyl protons can take up more than one position depending on

the direction of the hydrogen bonding in the overall structure. The implication of this can often be seen during the Fourier syntheses in one of the two following forms: two potential proton peaks pointing almost at each other or; a single peak obtained roughly in the middle of two oxygen atoms (donor-acceptor pair). Free refinements in these cases often lead to unreasonable bond lengths and angles, and can only be rectified by using appropriate constraints such as AFIX or DFIX. Only in the case of *BCYCT05* was the data was of good enough quality to allow the disorder of protons to be shown but DFIX was still necessary in order to keep the protons at reasonable distance to the oxygen atoms.

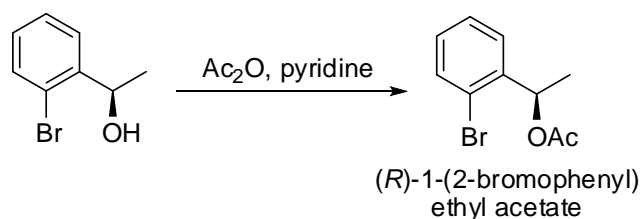
### Synthetic routes to 1–3

#### Procedure for preparation of 1

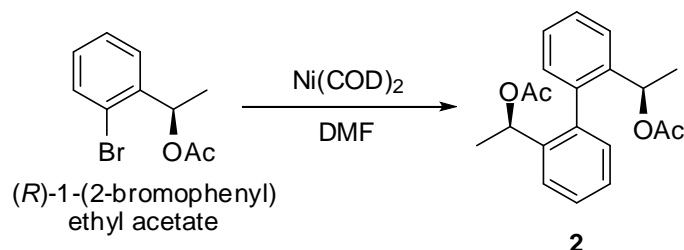


*(R)*-2-bromo- $\alpha$ -methylbenzenemethanol (1.00 g, 5 mmol) was added to a suspension of bis(1,5-cyclooctadiene)nickel(0) ( $\text{Ni}(\text{COD})_2$ ) (0.94 g, 3.4 mmol) in 6 mL DMF under nitrogen. The mixture was then heated at 45 °C for 16 hrs. After cooling to room temperature, the reaction was quenched by the addition of 5% aqueous HCl and extracted with  $\text{Et}_2\text{O}$ . The extract was dried with  $\text{MgSO}_4$  and purified with column chromatography (petroleum ether/ethyl acetate). After collecting the product portion, the solid was dissolved in warm  $\text{Et}_2\text{O}$ . Crystal was slowly formed upon cooling of the solution. The crystal was collected and then dried in vacuum to give **1** as colourless solid (0.67 g, 2.75 mmol, 55% yield).  $^1\text{H}$  NMR (400 MHz,  $\text{CDCl}_3$ ,  $\delta$ ): 1.40 (d,  $J = 6.4$  Hz, 6H), 2.71 (s, 2H), 4.57 (q,  $J = 6.4$  Hz, 2H), 7.11 (dd,  $J = 7.2$ , 0.8 Hz, 2H), 7.31 (td,  $J = 7.2$ , 1.2 Hz, 2H), 7.44 (td,  $J = 7.2$ , 0.8 Hz, 2H), 7.62 (dd,  $J = 8$ , 1.2 Hz, 2H).  $^{13}\text{C}$  NMR ( $\text{CDCl}_3$ ,  $\delta$ ): 23.5, 65.9, 125.3, 127.1, 128.2, 129.5, 139.0, 143.1.

#### Procedure for preparation of 2

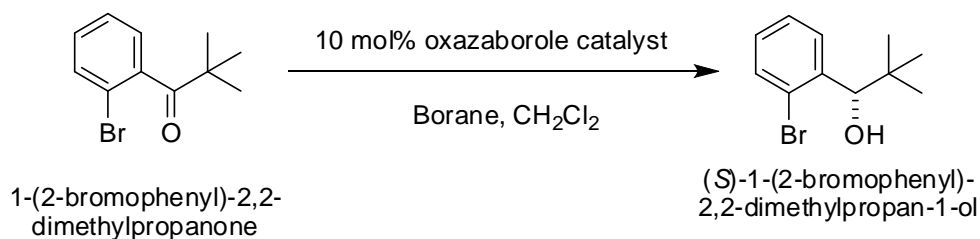


Acetic anhydride (2.1 mL, 22.2 mmol) was added dropwise to a solution of  $(R)$ -2-bromo- $\alpha$ -methylbenzenemethanol (1.68 g, 8.3 mmol) and pyridine (1.70 mL, 21.02 mmol) at 0 °C. The reaction mixture was allowed to stir at room temperature for 16 h. After quenching the reaction with water, the aqueous layer was extracted with CH<sub>2</sub>Cl<sub>2</sub> three times. The combined organic layers were washed with brine and then dried over MgSO<sub>4</sub>. The solvent was removed under reduced pressure to give an oily product (1.89 g, 7.78 mmol, 94% yield). <sup>1</sup>H NMR (400 MHz, CDCl<sub>3</sub>,  $\delta$ ): 1.52 (d,  $J$  = 6.4 Hz, 3H), 2.10 (s, 3H), 4.28 (q,  $J$  = 6.8 Hz, 1H), 7.14 (td,  $J$  = 8.0, 1.6 Hz, 1H), 7.32 (td,  $J$  = 7.2, 0.8 Hz, 1H), 7.44 (dd,  $J$  = 7.6, 1.6 Hz, 1H), 7.53 (dd,  $J$  = 8.0, 0.8 Hz, 1H). <sup>13</sup>C NMR (CDCl<sub>3</sub>,  $\delta$ ): 19.23, 36.33, 76.97, 117.71, 121.60, 122.41, 123.49, 126.55, 133.31, 156.46.



The coupling method for **2** is similar to the preparation of **1** except  $(R)$ -1-(2-bromophenyl)-ethyl acetate (2.62 g, 10.8 mmol), Ni(COD)<sub>2</sub> (2 g, 7.27 mmol) and 12 mL of DMF were used and the reaction was heated to 65 °C. The crude product was purified with column chromatography yielding colourless solid (2.6 g, 7.89 mmol, 73% yield). Two sets of peaks which are in a ratio of 53:47 were observed in <sup>1</sup>H NMR. The  $(R,R_a,R)$ -**2** isomer can be obtained as a pure isomeric solid by repeatedly recrystallization from warm Et<sub>2</sub>O solution of **2** (1.62 g, 4.97 mmol). <sup>1</sup>H NMR (400 MHz, CDCl<sub>3</sub>,  $\delta$ ): 1.36 (d,  $J$  = 6.4 Hz, 6H), 2.01 (s, 6H), 5.68 (q,  $J$  = 6.4 Hz, 2H), 7.26-7.27 (m, 2H), 7.34 (t,  $J$  = 7.6 Hz, 2H), 7.42 (t,  $J$  = 7.2 Hz, 2H), 7.57 (t,  $J$  = 7.6 Hz, 2H). <sup>13</sup>C NMR (CDCl<sub>3</sub>,  $\delta$ ): 21.25, 21.26, 69.43, 126.02, 127.55, 128.20, 130.28, 138.42, 139.32, 169.85. Isolation of the compound corresponding to another set of peak was not possible since the two compounds were equilibrated

### Procedure for preparation of **3**



1-(2-bromophenyl)-2,2-dimethylpropanone (1 g, 4.15 mmol) in CH<sub>2</sub>Cl<sub>2</sub> (0.2 mL) was added dropwise to a solution of oxazaborole-borane catalyst (0.06 g, 0.21 mmol) and borane-dimethyl sulfide (0.39 mL, 4.15 mmol) in CH<sub>2</sub>Cl<sub>2</sub> (0.26 mL) at 0 °C. The mixture was stirred at 0 °C for 6 h. After completion of reaction conversion, the reaction was precooled to -20 °C and then quenched carefully with dropwise addition of methanol (1 mL). The product was extracted with Et<sub>2</sub>O and dried with MgSO<sub>4</sub>. The crude product was purified with column chromatography yield colourless solid (0.81 g, 3.32 mmol, 80% yield). <sup>1</sup>H NMR (400 MHz, CDCl<sub>3</sub>, δ): 1.00 (s, 9H), 1.87 (d, *J* = 3.2 Hz, 2H), 5.00 (d, *J* = 3.6 Hz, 2H), 7.11 (td, *J* = 7.6, 1.6 Hz, 2H), 7.31 (t, *J* = 7.6 Hz, 2H), 7.53 (m, 4H). <sup>13</sup>C NMR (CDCl<sub>3</sub>, δ): 0.02, 25.91, 37.04, 124.10, 126.89, 128.72, 129.62, 132.59, 141.55. The enantiomeric purity was determined with HPLC with Whelk-O1 column (Hexane/*i*-propanol: 98/2; flow rate: 0.7 ml/min) and compared with a racemic mixture according to the elution orders with retention times, *t*<sub>S</sub> = 7.98 min and *t*<sub>R</sub> = 10.0 min) to be 95% ee. The absolute configuration was determined with X-ray crystallography (Fig. S4).

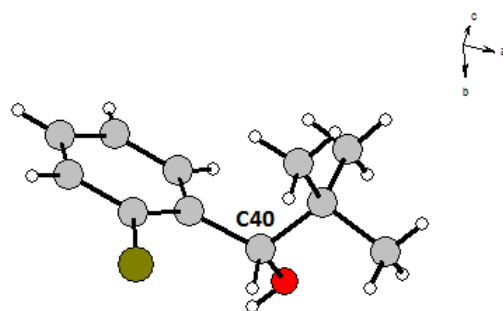


Fig. S4. X-ray crystallography of (S)-1-(2-bromophenyl)-2,2-dimethylpropan-1-ol showing (S) configuration at C40.

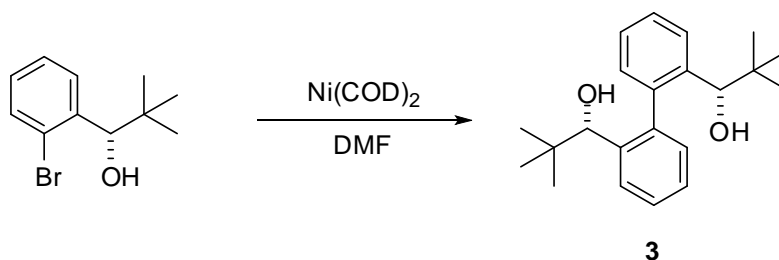
Table S4. Crystal data and structure refinement of (S)-1-(2-bromophenyl)-2,2-dimethylpropan-1-ol

Empirical formula	C <sub>11</sub> H <sub>15</sub> Br O
Formula weight	243.14
Temperature	296(2) K

---

Wavelength	0.71073 Å
Crystal system, space group	Monoclinic, P 21
Unit cell dimensions	a = 9.6636(24) Å    alpha = 90 ° b = 23.3522(52) Å    beta = 114.8955(147) ° c = 11.4105(27) Å    gamma = 90 °
Volume	2335.7(10) Å <sup>3</sup>
Z, Calculated density	8, 1.83 Mg/m <sup>3</sup>
Absorption coefficient	3.483 mm <sup>-1</sup>
F(000)	992
Crystal size	0.64 x 0.40 x 0.38 mm
θ range for data collection	2.63 to 24.71 °
Limiting indices	-11 ≤ h ≤ 11, -27 ≤ k ≤ 27, -13 ≤ l ≤ 13
Reflections collected / unique	25743 / 7887 [R(int) = 0.0513]
Completeness to θ	= 24.71, 99.7 %
Absorption correction	Semi-empirical from equivalents
Max. and min. transmission	0.3512 and 0.2140
Refinement method	Full-matrix least-squares on F <sup>2</sup>
Data / restraints / parameters	7887 / 1 / 481
Goodness-of-fit on F <sup>2</sup>	0.936
Final R indices [I > 2σ(I)]	R1 = 0.0435, wR2 = 0.0813
R indices (all data)	R1 = 0.0931, wR2 = 0.0937
Absolute structure parameter	-0.004(9)
Largest diff. peak and hole	0.284 and -0.310 e Å <sup>-3</sup>

---



The coupling method for **3** is similar to the preparation of **1** except (*S*)-1-(2-bromophenyl)-2,2-dimethylpropan-1-ol (1 g, 4.15 mmol), Ni(COD)<sub>2</sub> (0.86g, 3.13 mmol) and 5 mL DMF were used and the reaction was heated to 60 °C. The crude product was purified with column chromatography to give the product as colourless solid (0.47 g, 1.45 mmol, 35% yield). <sup>1</sup>H NMR (400 MHz, CDCl<sub>3</sub>, δ): 0.73 (s, 18H), 2.32 (d, *J* = 5.2 Hz, 2H), 4.28 (d, *J* = 5.2 Hz, 2H), 7.13 (dd, *J* = 7.6, 1.6 Hz, 2H), 7.31 (td, *J* = 7.6, 1.6 Hz, 2H), 7.37 (td, *J* = 7.5, 1.2 Hz, 2H), 7.58 (dd, *J* = 8, 1.6 Hz, 2H). <sup>13</sup>C NMR (CDCl<sub>3</sub>, δ): 0.02, 26.23, 36.58, 126.80, 126.96, 127.10, 130.70, 140.04, 140.95.

Table S5: Other relatively long C–H···π distances for crystal **1**, **3** and *rac*-**1**

Compound	D–H···A	D(H···A)	D(D···A)	∠(D–H···A)	Class
<b>1</b>	C14–H14A···Cg1	3.14	4.013(15)	158	inter-strand
	C17–H17A···Cg1	3.17	3.910(3)	133	intramolecular
	C27–H27A···Cg4	3.13	3.810(15)	128	intramolecular
	C25–H25A···Cg5	3.33	3.994(8)	130	Inter-strand
	C47–H47A···Cg5	3.14	3.810(16)	127	Intramolecular
	C23–H23A···Cg6	3.11	4.035(15)	173	Inter-strand
	C34–H34A···Cg6	3.23	4.091(15)	155	Inter-strand
	C37–H37A···Cg6	3.13	3.858(5)	133	Intramolecular
<b>3</b>	C10–H10B···Cg7	3.31	3.922(3)	123	Intermolecular
	C18–H18A···Cg7	3.34	4.027(2)	129	Intramolecular
	C21–H21B···Cg7	3.33	4.093(3)	138	Intramolecular
	C7–H7A···Cg8	3.23	3.944(2)	131	Intramolecular
	C9–H9B···Cg8	3.25	3.963(3)	132	Intramolecular
	C21–H21C···Cg8	3.31	3.927(3)	124	Intramolecular
<i>rac</i> - <b>1</b>	C75–H75A···Cg9	3.16	3.802(5)	127	Intermolecular
	C78–H78A···Cg10	3.19	3.917(5)	134	Intermolecular
	C55–H55A···Cg11	3.15	3.929(4)	143	Intermolecular
	C67–H67A···Cg12	3.33	4.032(3)	130	Intramolecular
	C14–H14A···Cg13	3.33	3.919(5)	124	Intermolecular
	C15–H15A···Cg13	3.20	3.849(4)	129	Intermolecular

C18–H18A···Cg14	3.09	3.840(6)	137	Intermolecular
C33–H33A···Cg14	3.16	4.064(4)	164	Inter-tetramer

Cg1, 4-6 are the centroids of aryl ring C21–C26, C11–C16, C31–C36 and C41–C46 of **1**, respectively. Cg7 and Cg8 are the centroids of aryl ring C1–C6 and C12–C17 of **3**, respectively. Cg9-14 are the centroids of aryl ring C21–C26, C31–C36, C41–C46, C51–C56, C61–C66 and C71–C76 of *rac-1*, respectively.

Table S6. Crystal data and structure refinement of **1–3** and *rac-1*

	<b>1</b>	<b>2</b>	<b>3</b>	<i>rac-1</i>
Empirical formula	C16 H18 O2	C20 H22 O4	C22 H30 O2	C16 H18 O2
Formula weight	242.30	326.38	326.46	242.30
Temperature	296(2) K	296(2) K	296(2) K	296(2) K
Wavelength	0.71073 Å	0.71073 Å	0.71073 Å	0.71073 Å
Crystal system, space group	Monoclinic, P 21	Orthorhombic, P 21 21 2	Tetragonal, P 43 21 2	Monoclinic, P 21/n
Unit cell dimensions	a = 7.7097(11) Å b = 19.332(2) Å c = 9.3678(12) Å α = 90° β = 93.144(9)° γ = 90°	a = 9.4979(4) Å b = 16.7194(6) Å c = 5.6273(2) Å α = 90° β = 90° γ = 90°	a = 9.8939(2) Å b = 9.8930(2) Å c = 40.1220(16) Å α = 90° β = 90° γ = 90°	a = 19.2144(6) Å b = 13.7947(4) Å c = 23.5076(7) Å α = 90° β = 106.5958(16)° γ = 90°
Volume	1394.1(3) Å <sup>3</sup>	893.61(6) Å <sup>3</sup>	3929.80(19) Å <sup>3</sup>	5971.3(3) Å <sup>3</sup>
Z, Calculated density	4, 1.154 Mg/m <sup>3</sup>	2, 1.213 Mg/m <sup>3</sup>	8, 1.104 Mg/m <sup>3</sup>	16, 1.078 Mg/m <sup>3</sup>
Absorption coefficient	0.075 mm <sup>-1</sup>	0.084 mm <sup>-1</sup>	0.069 mm <sup>-1</sup>	0.070 mm <sup>-1</sup>
F(000)	520	348	1424	2080
Crystal size	0.44 x 0.36 x 0.20 mm	0.42 x 0.36 x 0.14 mm	0.70 x 0.48 x 0.32 mm	0.56 x 0.56 x 0.26 mm
θ range for data collection	2.11 to 27.48°	3.82 to 27.59°	2.56 to 25.34°	1.21 to 25.00°
Limiting indices	-9 ≤ h ≤ 9, -24 ≤ k ≤ 25, -10 ≤ l ≤ 12	-12 ≤ h ≤ 11, -20 ≤ k ≤ 21, -7 ≤ l ≤ 7	-11 ≤ h ≤ 11, -11 ≤ k ≤ 11, -48 ≤ l ≤ 48	-22 ≤ h ≤ 21, -16 ≤ k ≤ 16, -27 ≤ l ≤ 27
Reflections collected / unique	13979 / 3245 [R(int) = 0.0351]	9507 / 2045 [R(int) = 0.0305]	33091 / 3584 [R(int) = 0.0791]	47181 / 10402 [R(int) = 0.0808]
Completeness to θ	99.1 %	99.6%	99.9 %	98.9%
Absorption	Semi-empirical	Semi-empirical	Semi-empirical	Semi-empirical

correction	from equivalents	from equivalents	from equivalents	from equivalents
Max. and min. transmission	0.9852 and 0.9679	0.7456 and 0.6054	0.9784 and 0.9536	0.9821 and 0.9620
Refinement method	Full-matrix least-squares on F <sup>2</sup>			
Data / restraints / parameters	3245 / 1 / 330	1229 / 0 / 112	3584 / 4 / 236	10402 / 5 / 675
Goodness-of-fit on F <sup>2</sup>	1.022	1.059	1.057	1.066
Final R indices [I>2σ(I)]	R1 = 0.0359, wR2 = 0.0767	R1 = 0.0336, wR2 = 0.0879	R1 = 0.0531, wR2 = 0.0894	R1 = 0.0861, wR2 = 0.2584
R indices (all data)	R1 = 0.0582, wR2 = 0.0864	R1 = 0.0426, wR2 = 0.0941	R1 = 0.0958, wR2 = 0.1012	R1 = 0.1185, wR2 = 0.3044
Extinction coefficient	0.032(3)	0.067(8)	0.0066(6)	-
Largest diff. peak and hole	0.126 and -0.114 e Å <sup>-3</sup>	0.172 and -0.129 e Å <sup>-3</sup>	0.126 and -0.144 e Å <sup>-3</sup>	0.421 and -0.271 e Å <sup>-3</sup>

#### 4. References:

1. Frisch, M. J. T., G. W.; Schlegel, H. B.; Scuseria, G. E.; Robb, M. A.; Cheeseman, J. R.; Montgomery, Jr., J. A.; Vreven, T.; Kudin, K. N.; Burant, J. C.; Millam, J. M.; Iyengar, S. S.; Tomasi, J.; Barone, V.; Mennucci, B.; Cossi, M.; Scalmani, G.; Rega, N.; Petersson, G. A.; Nakatsuji, H.; Hada, M.; Ehara, M.; Toyota, K.; Fukuda, R.; Hasegawa, J.; Ishida, M.; Nakajima, T.; Honda, Y.; Kitao, O.; Nakai, H.; Klene, M.; Li, X.; Knox, J. E.; Hratchian, H. P.; Cross, J. B.; Bakken, V.; Adamo, C.; Jaramillo, J.; Gomperts, R.; Stratmann, R. E.; Yazyev, O.; Austin, A. J.; Cammi, R.; Pomelli, C.; Ochterski, J. W.; Ayala, P. Y.; Morokuma, K.; Voth, G. A.; Salvador, P.; Dannenberg, J. J.; Zakrzewski, V. G.; Dapprich, S.; Daniels, A. D.; Strain, M. C.; Farkas, O.; Malick, D. K.; Rabuck, A. D.; Raghavachari, K.; Foresman, J. B.; Ortiz, J. V.; Cui, Q.; Baboul, A. G.; Clifford, S.; Cioslowski, J.; Stefanov, B. B.; Liu, G.; Liashenko, A.; Piskorz, P.; Komaromi, I.; Martin, R. L.; Fox, D. J.; Keith, T.; Al-Laham, M. A.; Peng, C. Y.; Nanayakkara, A.; Challacombe, M.; Gill, P. M. W.; Johnson, B.; Chen, W.; Wong, M. W.; Gonzalez, C.; and Pople, J. A. *Gaussian 03, Revision E.01*, Gaussian, Inc.: Wallingford CT, 2004.
2. S.-L. Li, T. Xiao, W. Xia, X. Ding, Y. Yu, J. Jiang, L. Wang, *Chem. Eur. J.* **2011**, *17*, 10716.
3. A. T. ten Cate, P. Y. W. Dankers, H. Kooijman, A. L. Spek, R. P. Sijbesma, E.

- W. Meijer, *J. Am. Chem. Soc.* **2003**, *125*, 6860.
4. K. Burgess, A. M. Porte, *Angew. Chem. Int. Ed. Engl.* **1994**, *33*, 1182.
  5. D. J. Mathre, A. S. Thompson, A. W. Douglas, K. Hoogsteen, J. D. Carroll, E. G. Corley, E. J. J. Grabowski, *J. Org. Chem.* **1993**, *58*, 2880.
  6. S. Rousseaux, M. Davi, J. Sofack-Kreutzer, C. Pierre, C. E. Kefalidis, E. Clot, K. Fagnou, O. Baudoin, *J. Am. Chem. Soc.* **2010**, *132*, 10706.
  7. G. M. Sheldrick, SADABS, Program for Empirical Absorption Correction of Area detector, University of Göttingen, Germany, **1997**.
  8. SAINT, Version 7.34, Bruker (**2007**). Bruker AXS Inc., Madison, Wisconsin, USA.
  9. G. M. Sheldrick, *Acta Crystallogr., Sect. A: Found. Crystallogr.*, **1990**, *46*, 467.
  10. G. M. Sheldrick, SHELX-97, Programme for Crystal Structure Refinement, University of Göttingen, 1990.
  11. A.L.Spek (**2005**) *PLATON, A Multipurpose Crystallographic Tool*, Utrecht University, Utrecht, The Netherlands.